Origin of magnetic anisotropy in doped Ce_2Co_{17} alloys

Liqin Ke,[1,*] D. A. Kukusta,[1,2] and Duane D. Johnson[1,3]

[1]*Ames Laboratory, U.S. Department of Energy, Ames, Iowa 50011, USA*
[2]*Institute for Metal Physics, 36 Vernadsky Street, 03142 Kiev, Ukraine*
[3]*Departments of Materials Science & Engineering and Physics, Iowa State University, Ames, Iowa 50011-2300*

Magnetocrystalline anisotropy (MCA) in doped Ce_2Co_{17} and other competing structures was investigated using density functional theory. We confirmed that the MCA contribution from dumbbell Co sites is very negative. Replacing Co dumbbell atoms with a pair of Fe or Mn atoms greatly enhance the uniaxial anisotropy, which agrees quantitatively with experiment, and this enhancement arises from electronic-structure features near the Fermi level, mostly associated with dumbbell sites. With Co dumbbell atoms replaced by other elements, the variation of anisotropy is generally a collective effect and contributions from other sublattices may change significantly. Moreover, we found that Zr doping promotes the formation of 1-5 structure that exhibits a large uniaxial anisotropy, such that Zr is the most effective element to enhance MCA in this system.

I. INTRODUCTION

The quest for novel high-energy permanent magnet without critical elements continues to generate great interest [1]. While a rare-earth-free permanent magnet is appealing, developing a Ce-based permanent magnet is also very attractive, because among rare-earth elements Ce is most abundant and relatively cheap. Among Ce-Co systems, Ce_2Co_{17} has always attracted much attention due to its large Curie temperature T_C and magnetization M. The weak point of Ce_2Co_{17} is its rather small easy-axis magnetocrystalline anisotropy (MCA), which must be improved to use as an applicable permanent magnet.

The anisotropy in Ce_2Co_{17}, in fact, can be improved significantly through doping with various elements. Experimental anisotropy field H_A measurements by dopant and stoichiometry are shown in Fig. 1. This anisotropy enhancement has been attributed to the preferential substitution effects of doping atoms [2,3]: (i) The four nonequivalent Co sites contribute differently [4] to the magnetic anisotropy in Ce_2Co_{17}. Two out of the 17 Co atoms occupy the so-called dumbbell sites and have a very negative contribution to uniaxial anisotropy, leading to the small overall uniaxial anisotropy; (ii) Doping atoms preferentially replace the dumbbell sites first, eliminating their negative contribution and increasing the overall uniaxial anisotropy. The above explanation is supported by the observation that with many different dopants, the anisotropy field in $Ce_2T_xCo_{17-x}$ shows a maximum around $x = 2$. This corresponds to the number of dumbbell sites in one formula unit [5].

Numerous experimental efforts have explored the preferential substitution effect and site-resolved anisotropy. Streever [12] studied the site contribution to the MCA in Ce_2Co_{17} using nuclear magnetic resonance and concluded that the dumbbell sites in Ce_2Co_{17} have a very negative contribution to uniaxial anisotropy. Neutron scattering or Mössbauer studies have suggested that Fe [12–15], Mn [16], and Al [7,17,18] atoms prefer to substitute at dumbbell sites.

However, it is not clear whether only the preferential substitution effect plays a role in H_A enhancement for all

doping elements. For elements such as Zr, Ti, and Hf, the substitution preference is not well understood. Replacing the dumbbell Co atoms with a pair of large atoms may not always be the only energetically favorable configuration. For Mn and Fe, known to substitute at dumbbell sites, the elimination of negative contributions at those sites may explain the increase of magnetocrystalline anisotropy energy (MAE). It is yet unclear why different elements give a different amplitude of MAE enhancement or what mechanism provides this enhancement. For permanent magnet application, Fe and Mn are particularly interesting because they improve the anisotropy while preserving the magnetization with $x < 2$. Other dopants quickly reduce the magnetization and Curie temperature. Further tuning of magnetic properties for compounds based on Fe-or-Mn-doped Ce_2Co_{17} would benefit from this understanding.

In this work, we use density functional theory (DFT) to investigate the origin of the MAE enhancement in doped Ce_2Co_{17}. By evaluating the on-site spin-orbit coupling (SOC) energy [19,20], we resolved anisotropy into contributions from atomic sites, spins, and orbital pairs. Furthermore, we explained the electronic-structure origin of MAE enhancement.

II. CALCULATION DETAILS

A. Crystal structure

Ce_2Co_{17} crystallizes in the hexagonal Th_2Ni_{17}-type ($P6_3/mmc$, space group no. 194) structure or the rhombohedral $Zn_{17}Th_2$-type ($R\bar{3}mh$, space group no. 166) structure, depending on growth condition and doping [10]. As shown in Fig. 2, both 2-17 structures can be derived from the hexagonal $CaCu_5$-type ($P6/mmm$ space group 191) structure with every third Ce atom being replaced by a pair of Co atoms (referred to as dumbbell sites). The two 2-17 structures differ only in the spatial ordering of the replacement sites. In the $CeCo_5$ cell, a Ce atom occupies the $1a(6/mmm)$ site and two Co atoms occupy the $2c(\bar{6}m2)$ site, together forming a Ce-Co basal plane. Three Co atoms occupy the $3g(mmm)$ sites and form a pure Co basal plane. The primitive cell of hexagonal $Ce_2Co_{17}(H-Ce_2Co_{17})$ contains two formula units while the rhombohedral $Ce_2Co_{17}(R-Ce_2Co_{17})$ contains one. The Co
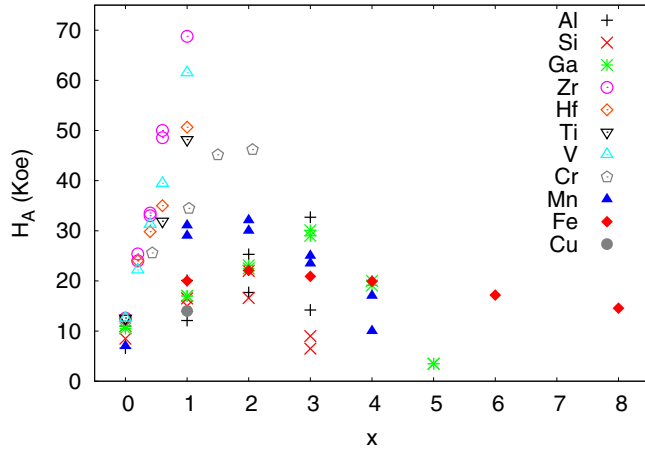
*Corresponding author: liqinke@ameslab.gov

FIG. 1. Experimental anisotropy fields H_A in $Ce_2T_xCo_{17-x}$ with T = Al [6,7], Si [6,8], Ga [6,9], Zr [10], Hf [10], V [5], Cr [5], Mn [5,11], Fe [5], and Cu [5].

atoms are divided into four sublattices, denoted by Wyckoff sites $18h$, $18f$, $9d$, and $6c$ in the rhombohedral structure, and $12k$, $12j$, $6g$, and $4f$ in the hexagonal structure. The $6c$ and $4f$ sites are the dumbbell sites. In the R structure, Ce atoms form -Ce-Ce-Co-Co- chains with Co atoms along the z axis. The H structure has two inequivalent Ce sites, denoted as $2c$ and $2b$, respectively. Along the z direction, Ce_{2b} form pure -Ce- atoms chains and Ce_{2c} form -Ce_{2c}-Co-Co- chains with Co dumbbell sites.

B. Computational methods

We carried out first-principles DFT calculations using the Vienna *ab initio* simulation package (VASP) [21,22] and a variant of the full-potential linear muffin-tin orbital (LMTO) method [23]. We fully relaxed the atomic positions and lattice parameters, while preserving the symmetry using VASP. The nuclei and core electrons were described by the projector

augmented-wave potential [24] and the wave functions of valence electrons were expanded in a plane-wave basis set with a cutoff energy of 520 eV. The generalized gradient approximation of Perdew, Burke, and Ernzerhof was used for the correlation and exchange potentials.

The MAE is calculated below as $K = E_{100} - E_{001}$, where E_{001} and E_{100} are the total energies for the magnetization oriented along the [001] and [100] directions, respectively. Positive (negative) K corresponds to uniaxial (planar) anisotropy. The spin-orbit coupling is included using the second-variation procedure [25,26]. The k-point integration was performed using a modified tetrahedron method with Blöchl corrections. To ensure the convergence of the calculated MAE, dense k meshes were used. For example, we used a 16^3 k-point mesh for the calculation of MAE in $R-Ce_2Co_{17}$. We also calculated the MAE by carrying out all-electron calculations using the full-potential LMTO (FP-LMTO) method to check anisotropy results. To decompose the MAE, we evaluate the anisotropy of the scaled on-site SOC energy $K_{so} = \frac{1}{2}\langle V_{so}\rangle_{100} - \frac{1}{2}\langle V_{so}\rangle_{001}$. According to second-order perturbation theory [19,20], $K \approx \sum_i K_{so}(i)$, where i indicates the atomic sites. Unlike K, which is calculated from the total energy difference, K_{so} is localized and can be decomposed into sites, spins, and subband pairs [19,20].

III. RESULTS AND DISCUSSION

A. Ce_2Co_{17}

Atomic spin and orbital magnetic moments in Ce_2Co_{17} and $CeCo_5$ are summarized in Table I. The calculated magnetization are 26.1–26.9 μ_B/f.u. in Ce_2Co_{17} and 7.14 μ_B/f.u. in $CeCo_5$, which agree with experiments [6]. Ce spin couples antiferromagneticlly with the Co spin. The orbital magnetic moment of Ce is antiparallel to its spin, which reflects Hunds' third rule. In the Ce-Co plane of Ce_2Co_{17} the Ce atoms are partially replaced by dumbbell Co atoms and this leads to an increased moment for the Co atoms (in that plane) as compared to $CeCo_5$. The dumbbell sites have the largest magnetic
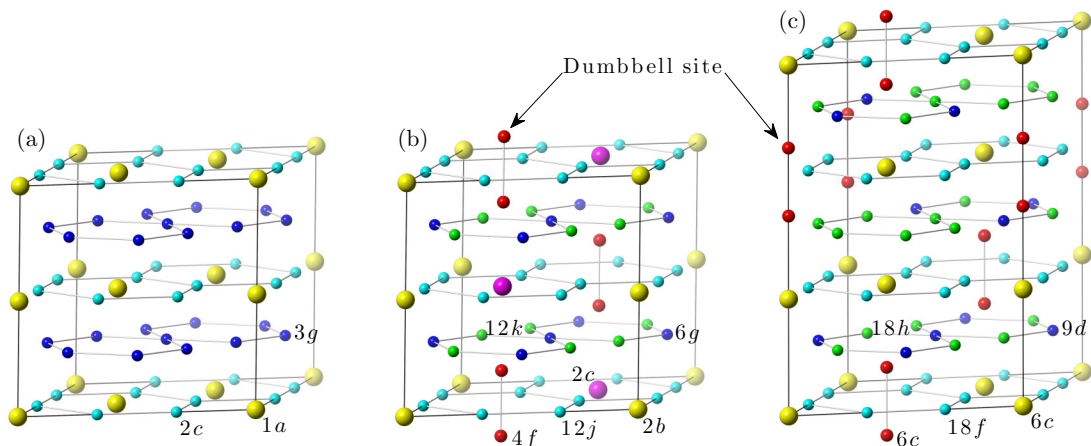

FIG. 2. Schematic crystal structures of (a) $CeCo_5$, (b) hexagonal $H-Ce_2Co_{17}$, and (c) rhombohedral $R-Ce_2Co_{17}$. Ce atoms are indicated with large (yellow or magenta colored) spheres. Co atoms are denoted by Wyckoff sites. Dumbbell (red) sites are denoted in $H-Ce_2Co_{17}$ ($4f$ sites) and in $R-Ce_2Co_{17}$ ($6c$ sites), and indicated further by arrows and label. We use larger cells for $CeCo_5$ and $R-Ce_2Co_{17}$ to compare with $H-Ce_2Co_{17}$.

TABLE I. Atomic spin m_s and orbital m_l magnetic moments (μ_B/atom) in CeCo$_5$, $R-$Ce$_2$Co$_{17}$, and $H-$Ce$_2$Co$_{17}$. Atomic sites are grouped to reflect how the 2-17 structure arises from the 1-5 structure. Measured magnetization is 26.5 μ_B/f.u. in $H-$Ce$_2$Co$_{17}$ at $5K$ [6] and 7.12 μ_B/f.u. in CeCo$_5$ [27]. Dumbbell sites are denoted as $6c$ and $4f$ in $R-$Ce$_2$Co$_{17}$ and $H-$Ce$_2$Co$_{17}$, respectively.

CeCo$_5$	$2c$	$3g$			$1a$ (Ce)	Total
m_s	1.33	1.44			-0.76	6.22
m_l	0.14	0.12			0.30	0.92
$R-$Ce$_2$Co$_{17}$	$18f$	$18h$	$9d$	$6c$	$6c$(Ce)	Total
m_s	1.53	1.43	1.52	1.65	-0.85	23.94
m_l	0.10	0.09	0.07	0.07	0.35	2.17
$H-$Ce$_2$Co$_{17}$	$12j$	$12k$	$6g$	$4f$	$2c$(Ce) $2b$(Ce)	Total
m_s	1.56	1.51	1.51	1.65	-0.84 $\quad-0.90$	24.50
m_l	0.11	0.10	0.08	0.07	0.38 $\quad$ 0.42	2.43

moment due to its relatively large volume. Calculation shows Ce$_2$Co$_{17}$ has a small uniaxial anisotropy, 0.13 meV/f.u. (0.09 MJm^{-3}) and 0.47 meV/f.u. (0.30 MJm^{-3}) for $R-$Ce$_2$Co$_{17}$ and $H-$Ce$_2$Co$_{17}$, respectively. The experimental values fall slightly above the calculated ones; see Fig. 3.

To understand the low uniaxial anisotropy in Ce$_2$Co$_{17}$, we resolve the anisotropy into atomic sites by evaluating K_{so}. The anisotropy contributions in Ce$_2$Co$_{17}$ can be divided into three groups: the pure Co plane ($3g$ in CeCo$_5$, $12k + 6g$ in $H-$Ce$_2$Co$_{17}$, or $18h + 9d$ in $R-$Ce$_2$Co$_{17}$), the Ce-Co plane, and the Co dumbbell pairs. We found that the MAE contributions from these three groups in the two 2-17 structures are very similar: the dumbbell Co sites have a very negative contribution to uniaxial anisotropy; the pure-Co basal plane has a negligible or even slightly negative contribution to the uniaxial anisotropy; only the Ce-Co basal plane provides
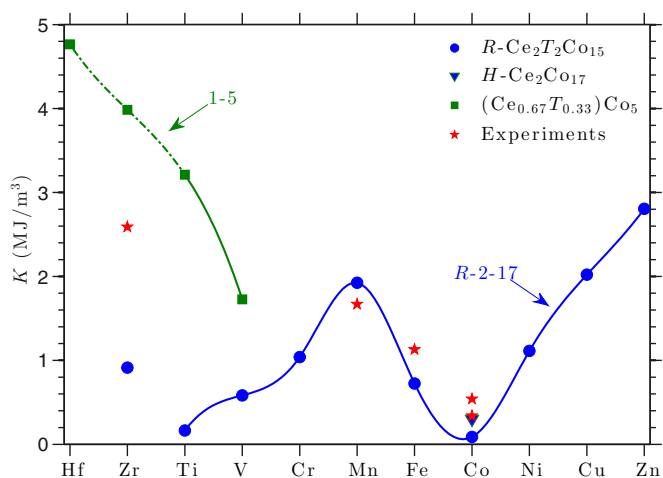
uniaxial anisotropy in Ce$_2$Co$_{17}$. The two inequivalent Ce sites contribute differently to the uniaxial anisotropy in $H-$Ce$_2$Co$_{17}$ structure. Ce($2b$) supports uniaxial anisotropy while Ce($2c$) moment prefer to be in-plane. However, the total contribution from the two Ce sites is positive, as in the R structure.

Intrinsic magnetic properties and the effect of doping on them are very similar in the two 2-17 structures. We only discuss the results calculated using the R structure because it has a smaller primitive cell than the H structure, and the most interesting substituents, Fe and Mn, promote its formation [5].

B. MAE in Ce$_2T_2$Co$_{15}$

We first calculate the MAE in Ce$_2T_2$Co$_{15}$ with a variety of doping elements T, by assuming the pair of Co dumbbell atoms is replaced by a pair of doping atoms. The calculated MAE as a function of doping elements for $T =$ Zr and $3d$ elements is shown in Fig. 3. Fe and Mn doping increase the MAE, aligning with with experimental results. However, the MAE calculated for light d elements $T =$ Ti, V, and Zr are rather small while experiments show that large enhancements of MAE can be achieved with a small amount of doping of those elements. Interestingly, large MAE values are obtained in Ce$_2T_2$Co$_{15}$ with $T =$ Cu or Zn. In fact, a small amount of Cu are often added to the alloy to improve the coercivity and the enhancement had been interpreted as precipitation hardening by Cu. It may not be unexpected that the enhancement of coercivity may also partially arise from the increase of MAE, although Cu atoms had been reported to randomly occupy all Co sites [17]. Moreover, the trend of MAE in Ce$_2T_2$Co$_{15}$, as shown in Fig. 3, is rather generic. We also found the similar trend in Y$_2T_2$Co$_{15}$ and La$_2T_2$Co$_{15}$, MAE increases with $T =$ Mn, or late $3d$ elements. Calculations using FP-LMTO method also shows similar trends of MAE.

The total K_{so}, its contribution from the dumbbell site, and the other sublattices' contributions are shown in Fig. 4. Total K_{so} closely follows K for all doping elements, thus validating our use of K_{so} to resolve the MAE and understand its origin. As shown in Fig. 4, the Co dumbbell sublattice in $R-$Ce$_2$Co$_{17}$
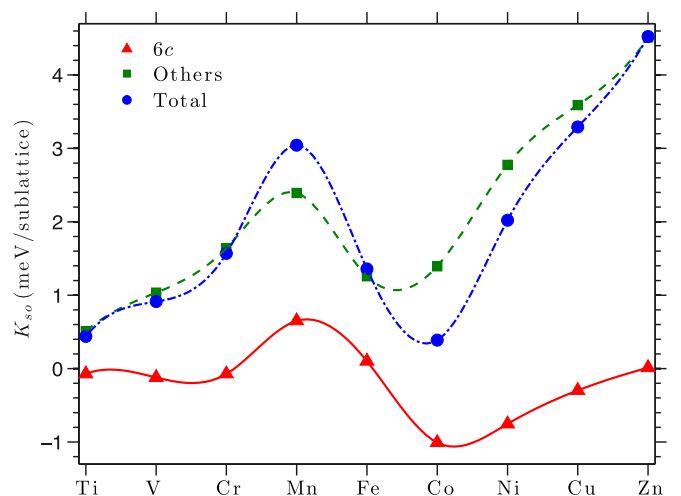

FIG. 3. Magnetic anisotropy in Ce$_2T_2$Co$_{15}$ and Ce$_{0.66}T_{0.33}$Co$_5$ with $T =$ Ti, V, Cr, Mn, Fe, Co, Ni, Cu, Zr, and Hf. In Ce$_2T_2$Co$_{15}$, T atoms occupy the dumbbell sublattice. The Ce$_{0.66}T_{0.33}$Co$_5$ structure was obtained by replacing the pair of dumbbell Co atoms in the original Ce$_2$Co$_{17}$ with a single T atom. K values derived from experimental H_A measurements [5,11] by using $K = \frac{1}{2}\mu_0 M_s H_A$ are also shown.

FIG. 4. Anisotropy of the scaled onsite SOC energy K_{so} in Ce$_2T_2$Co$_{15}$ and its contributions from the dumbbell sublattice $T(6c)$ and the rest sublattices.

has a very negative contribution to the uniaxial anisotropy $K_{so}(6c) = 1$ meV/f.u. (0.5 meV/atom). Replacing Co with other $3d$ elements decreases or eliminates this negative contribution, or even make it positive, as with $T =$ Mn. For the dumbbell site contributions, only four elements with large magnetic moments (all ferromagneticlly couple to Co sublattice), Mn, Fe, Co, and Ni, have nontrivial contributions. Atoms on both ends of the $3d$ elements have negligible contributions to the uniaxial anisotropy as expected. Although Cu and Zn have the largest SOC constants among $3d$, they are nearly nonmagnetic; hence, they barely contribute to the MAE itself [20]. The light elements Ti, V, and Cr have small spin moments between 0.36 and 0.55 μ_B (antiparallel to the Co sublattice) and smaller SOC constants, together resulting in a small $K_{so}(T)$.

Although the dumbbell site contribution dominates the MAE enhancement for $T =$ Fe and Mn, it is obvious that the variation of MAE is a collective effect, especially for $T =$ Cu, or Zn. While the -1 meV/f.u. negative contribution from the dumbbell sublattice is eliminated with $T =$ Cu and Zn, the contributions from the rest sublattices increase by about 2 and 3 meV/f.u., respectively. Similarly, for the doping of nonmagnetic Al atoms, the calculated MAE in $Ce_2Al_2Co_{15}$ has a large value of $K = 3.8$ meV/f.u.. Experimentally, Al atoms had been found to prefer to occupy the dumbbell site and also increase the uniaxial anisotropy [7,17]. MAE often depends on subtle features of the band structure near the Fermi level; therefore, the collective effect of MAE variation should be expected for a metallic system [28]. The modification of one site, such as doping, unavoidably affects the electronic configuration of other sites and their contribution to MAE.

C. Origin of MAE in $Ce_2T_2Co_{15}$ with $T =$ Fe and Mn

We found that all dopings except Fe and Mn decrease the magnetization, which is consistent with the experiments by Fujji *et al.* [5], and Schaller *et al.* [29]. $Ce_2Fe_2Co_{15}$ and $Ce_2Mn_2Co_{15}$ have slightly larger magnetization than Ce_2Co_{17} by 5% and 8%, respectively. It is worth noting that experimental result on Mn doping is rather inconclusive. A slight decrease of magnetization with Mn doping has also been reported [11].

Sublattice-resolved K_{so} in $Ce_2T_2Co_{15}$ for $T =$ Co, Fe, and Mn are shown in Fig. 5(a). The dominant enhancement of MAE are from the dumbbell site, although contributions from other sublattices also vary with T. To understand this enhancement of K_{so} from the dumbbell sites, we further resolved K_{so} into contributions from allowed transitions between all pairs of subbands. The dumbbell sites have $3m$ symmetry. Without considering SOC, five d orbitals on T sites split into three groups: d_{z^2} state, degenerate (d_{yz}, d_{xz}) states, and degenerate $(d_{xy}, d_{x^2-y^2})$ states. Equivalently, they can be labeled as $m = 0$, $m = \pm 1$, and $m = \pm 2$ using cubic harmonics. $K_{so}(T)$ can be written as [20]

$$K_{so}(T) = \frac{\xi^2}{4}\left(4\chi_{22}^{\epsilon} + \chi_{11}^{\epsilon} - 3\chi_{01}^{\epsilon} - 2\chi_{12}^{\epsilon}\right), \qquad (1)$$

where ξ is the SOC constant and $\chi_{mm'}^{\epsilon}$ is the difference between the spin-parallel and spin-flip components of orbital
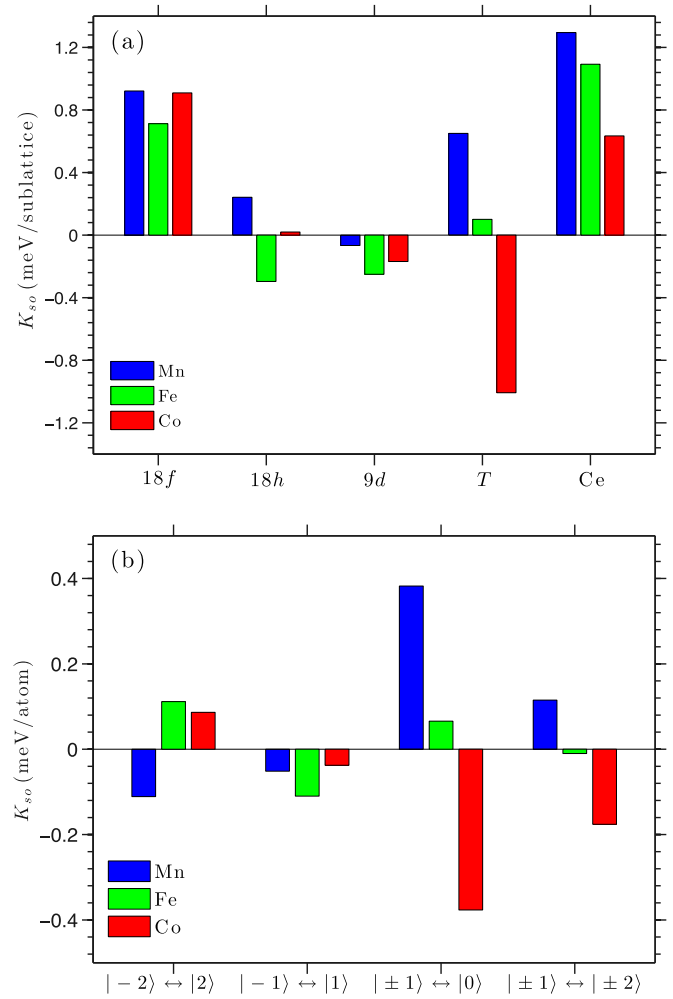

FIG. 5. (a) Site-resolved anisotropy of the onsite SOC energy K_{so} and (b) orbital-resolved $K_{so}(6c)$ in $Ce_2Co_{17-x}T_x$ with $T =$ Co, Fe, and Mn.

pair susceptibility. It can be written as

$$\chi_{mm'}^{\epsilon} = \chi_{mm'}^{\uparrow\uparrow} + \chi_{mm'}^{\downarrow\downarrow} - \chi_{mm'}^{\uparrow\downarrow} - \chi_{mm'}^{\downarrow\uparrow}. \qquad (2)$$

Contributions to $K_{so}(T)$ resolved into transitions between pairs of subbands are shown in Fig. 5(b). The four groups of transitions correspond to the four terms in Eq. (1). The dominant effect is from $|0\rangle \leftrightarrow |\pm 1\rangle$, namely the transitions between d_{z^2} and $(d_{yz}|d_{xz})$ orbitals. This contribution is negative for $T =$ Co, nearly disappears for $T =$ Fe, and even becomes positive and large for $T =$ Mn.

The interesting dependence of $|0\rangle \leftrightarrow |\pm 1\rangle$ contribution on T can be understood by investigating how the electronic structure changes with different T elements. The sign of the MAE contribution from transitions between a pair of subbands $|m,\sigma\rangle$ and $|m',\sigma'\rangle$ is determined by the spin and orbital character of the involved orbitals [20,30]. Inter-$|m|$ transitions $|0\rangle \leftrightarrow |\pm 1\rangle$ promote easy-plane anisotropy within the same spin channel and easy-axis anisotropy when between different spin channels.

The scalar-relativistic partial densities of states (PDOS) projected on the dumbbell site are shown in Fig. 6. For $T =$ Co, the majority spin channel is nearly fully occupied and has very

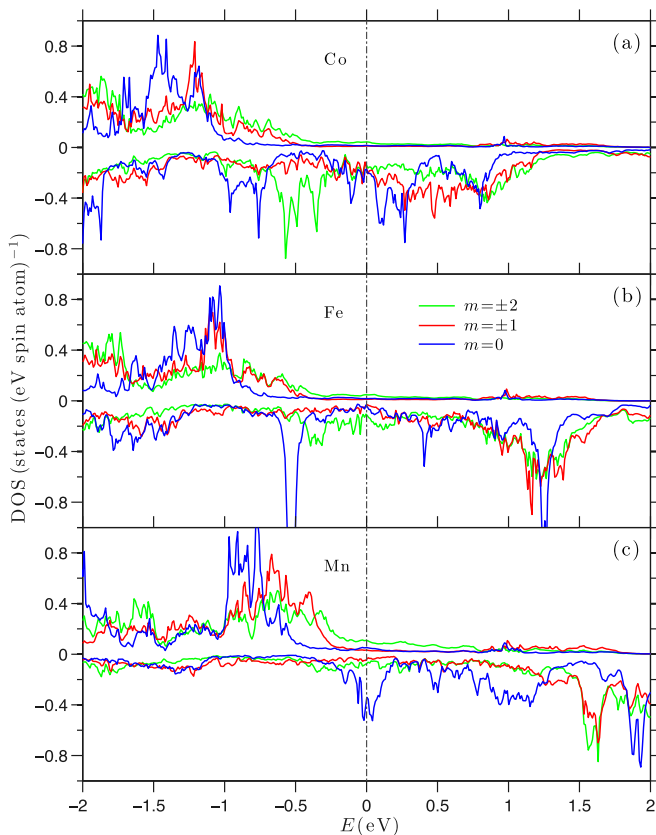FIG. 6. The scalar-relativistic partial density of states projected on the 3d states of T sites in R–Ce$_2$T$_2$Co$_{15}$ with T = Co, Fe, and Mn. T atoms occupy the dumbbell ($6c$) sites.

small DOS around the Fermi level, while the minority spin channel has a larger DOS. The transitions between d_{z^2} and (d_{yz},d_{xz}) states across the Fermi level and within the minority spin channel, namely $|0, \downarrow\rangle \leftrightarrow |\pm 1, \downarrow\rangle$, promote the easy-plan anisotropy. For T = Fe, the PDOS of d_{z^2} and (d_{yz},d_{xz}) are rather small near the Fermi level in both spin channels and the net contribution from $|0\rangle \leftrightarrow |\pm 1\rangle$ becomes negligible. For T = Mn, the Fermi level intersects a large peak of the d_{z^2} state at the Fermi level in the minority spin channel. The spin-flip transitions $|0, \downarrow\rangle \leftrightarrow |\pm 1, \uparrow\rangle$ give rise to a large positive contribution to uniaxial anisotropy.

D. Zr, Ti, and Hf doping in Ce$_2$Co$_{17}$

The failure to reproduce high anisotropy introduced by other dopants, such as Zr, Ti, and V, is likely due to our oversimplified assumption that a pair of T atoms always replaces a pair of Co dumbbell atoms. Unlike Fe and Mn, the site occupancy preference for those dopants is not well understood [31]. Considering Zr doping most effectively enhanced H_A in experiments, here we focus on Zr doping.

Both volume and chemical effects likely play important roles in substitution site preference. To have a better understanding of the Zr site preference, we calculated the formation energy of Ce$_2$ZrCo$_{16}$ with the Zr atom occupying one of the four nonequivalent Co sites and found that Zr also prefers to occupy the dumbbell sites—likely due to the relatively large volume around the dumbbell sites. The

formation energies are higher by 39, 58, and 81 meV/atom when Zr occupies the 18f, 18h, or 9d sites, respectively. Considering Zr atoms are relatively large, we investigated another scenario by replacing the pair of Co dumbbell atoms with a single Zr atom, as suggested by Larson and Mazin [31]. Indeed, this latter configuration of Ce$_2$ZrCo$_{15}$ has the lowest formation energy, which is 3 meV/atom lower than that of Ce$_2$Zr$_2$Co$_{15}$ and 1 meV/atom lower than Ce$_2$Co$_{16}$Zr (with Zr replacing one of the two dumbbell Co atoms in Ce$_2$Co$_{17}$). That is, with Zr additions the CeCo$_5$ structure is preferred over the Ce$_2$Co$_{17}$-based structure. The resulting Ce$_2$ZrCo$_{15}$ has a 1-5 structure (Ce$_{0.67}$Zr$_{0.33}$)Co$_5$, with one-third of the Ce in the CeCo$_5$ structure, shown in Fig. 2(a), replaced by Zr atoms. Hence, the formation energy calculation indicate that the realized structure is likely a mix of 2-17 and 1-5 structures. Interestingly, this may be related to experimental observations that successful 2-17 magnets usually have one common microstructure, i.e., separated cells of 2-17 phase surrounded by a thin shell of a 1-5 boundary phase, and Zr, Hf, or Ti additions promote the formation of such structure [3].

The calculated anisotropy in Ce$_2$ZrCo$_{15}$, or equivalently (Ce$_{0.67}$Zr$_{0.33}$)Co$_5$, is about 4 MJm^{-3} and much larger than that of Ce$_2$Zr$_2$Co$_{15}$. Analysis of K_{so} reveals that not only is the negative contribution from the previous dumbbell sites eliminated, but more importantly, the pure Co plane becomes very uniaxial. For T = V and Ti, the calculated MAE in this configuration is also much larger than that of Ce$_2$T$_2$Co$_{15}$, as shown in Fig. 3. Similarly, a large MAE of 2.41 meV/f.u. was obtained for (Ce$_{0.67}$Hf$_{0.33}$)Co$_5$.

IV. CONCLUSION

Using density functional theory, we investigated the origin of anisotropy in doped Ce$_2$Co$_{17}$. We confirmed that the dumbbell sites have a very negative contribution to the MAE in Ce$_2$Co$_{17}$ with a value about 0.5 meV/atom. The enhancement of MAE due to Fe and Mn doping agrees well with experiments, which can be explained by the preferential substitution effect because the enhancement is dominated by dumbbell sites. The transitions between the d_{z^2} and ($d_{yz}|d_{xz}$) subbands on dumbbell sites are responsible for the MAE variation, and these transitions can be explained by the PDOS around the Fermi level, which in turn depends on the element T occupying on the dumbbell site. For Zr doping, the calculated formation energy suggests that the real structure is likely a mix of 2-17 and 1-5 structures, and the resulted 1-5 structure has a large anisotropy, which may explain the large MAE enhancement observed in experiments. The variation of MAE due to doping is generally a collective effect. Doping on dumbbell sites may significantly change the contributions from other sublattices and then the overall anisotropy. It is worth investigating other nonmagnetic elements with a strong dumbbell site substitution preference because it may increase the total anisotropy in this system by increasing the contributions from other sublattices.

[1] R. McCallum, L. Lewis, R. Skomski, M. Kramer, and I. Anderson, Annu. Rev. Mater. Res. **44**, 451 (2014).

[2] K. H. J. Buschow, Rep. Prog. Phys. **40**, 1179 (1977).

[3] K. Strnat, in *Handbook of Ferromagnetic Materials* (Elsevier, Amsterdam, 1988), Vol. 4, pp. 131–209.

[4] S. Yajima, M. Hamano, and H. Umebayashi, J. Phys. Soc. Jpn. **32**, 861 (1972).

[5] H. Fujii, M. V. Satyanarayana, and W. E. Wallace, J. Appl. Phys. **53**, 2371 (1982).

[6] S. Hu, X. Wei, D. Zeng, X. Kou, Z. Liu, E. Brck, J. Klaasse, F. de Boer, and K. Buschow, J. Alloys Compd. **283**, 83 (1999).

[7] B. Shen, Z. Cheng, S. Zhang, J. Wang, B. Liang, H. Zhang, and W. Zhan, J. Appl. Phys. **85**, 2787 (1999).

[8] X. Wei, S. Hu, D. Zeng, X. Kou, Z. Liu, E. Brück, J. Klaasse, F. de Boer, and K. Buschow, Physica B: Condensed Matter **262**, 306 (1999).

[9] X. Wei, S. Hu, D. Zeng, X. Kou, Z. Liu, E. Brck, J. Klaasse, F. de Boer, and K. Buschow, J. Alloys Compd. **279**, 301 (1998).

[10] H. Fujii, M. Satyanarayana, and W. Wallace, Solid State Commun. **41**, 445 (1982).

[11] Z. Sun, S. Zhang, H. Zhang, J. Wang, and B. Shen, J. Phys.: Condens. Matter **12**, 2495 (2000).

[12] R. L. Streever, Phys. Rev. B **19**, 2704 (1979).

[13] J. Deportes, D. Givord, R. Lemaire, H. Nagai, and Y. Yang, J. Less Common Metals **44**, 273 (1976).

[14] R. Perkins and P. Fischer, Solid State Commun. **20**, 1013 (1976).

[15] P. Gubbens and K. Buschow, Phys. Status Solidi A **34**, 729 (1976).

[16] A. Kuchin, A. Pirogov, V. Khrabrov, A. Teplykh, A. Ermolenko, and E. Belozerov, J. Alloys Compd. **313**, 7 (2000).

[17] K. Inomata, Phys. Rev. B **23**, 2076 (1981).

[18] C. de Groot, F. de Boer, K. Buschow, Z. Hu, and W. Yelon, J. Alloys Compd. **233**, 188 (1996).

[19] V. Antropov, L. Ke, and D. Åberg, Solid State Commun. **194**, 35 (2014).

[20] L. Ke and M. van Schilfgaarde, Phys. Rev. B **92**, 014423 (2015).

[21] G. Kresse and J. Hafner, Phys. Rev. B **47**, 558 (1993).

[22] G. Kresse and J. Furthmüller, Phys. Rev. B **54**, 11169 (1996).

[23] M. Methfessel, M. van Schilfgaarde, and R. Casali, in *Lecture Notes in Physics*, edited by H. Dreysse (Springer-Verlag, Berlin, 2000), Vol. 535.

[24] G. Kresse and D. Joubert, Phys. Rev. B **59**, 1758 (1999).

[25] D. Koelling and B. Harmon, J. Phys. C **10**, 3107 (1977).

[26] A. B. Shick, D. L. Novikov, and A. J. Freeman, Phys. Rev. B **56**, R14259(R) (1997).

[27] M. Bartashevich, T. Goto, A. Korolyov, and A. Ermolenko, J. Magn. Magn. Mater. **163**, 199 (1996).

[28] L. Ke and D. D. Johnson, Phys. Rev. B **94**, 024423 (2016).

[29] H. Schaller, R. Craig, and W. Wallace, J. Appl. Phys. **43**, 3161 (1972).

[30] G. H. O. Daalderop, P. J. Kelly, and M. F. H. Schuurmans, Phys. Rev. B **50**, 9989 (1994).

[31] P. Larson and I. I. Mazin, Phys. Rev. B **69**, 012404 (2004).